computation

MDPI

Article

Competing Risks with Common Shocks: Joint Survival, Copulas, Censoring, Frailty, and Marshall–Olkin Models

Cristian David Correa-Álvarez [1,*], Mario Cesar Jarramillo-Elorza [2] and Osnamir Elias Bru-Cordero [3]

[1] Departamento de Matemáticas y Estadística, Universidad Nacional de Colombia, Sede Manizales, Manizales 170003, Colombia
[2] Departamento de Estadística, Universidad Nacional de Colombia, Sede Medellin, Medellin 050030, Colombia; mcjarami@unal.edu.co
[3] Dirección Académica, Universidad Nacional de Colombia, Sede de La Paz, Cesar 202010, Colombia; oebruc@unal.edu.co
* Correspondence: crdcorreaal@unal.edu.co

Abstract

This study examines likelihood-based estimation of the joint survival function $S(t_1, t_2) = \Pr\{T^{(1)} > t_1, T^{(2)} > t_2\}$ for systems with two competing failure modes observed under right censoring. Rather than introducing a new distributional family, the study compares established dependence mechanisms within a common observed-data framework. Exponential and Weibull margins are combined with three types of dependence: Archimedean copulas, represented by the Gumbel and Clayton families; shared gamma frailty, used to model latent measurement-level heterogeneity; and Marshall–Olkin extensions, used to represent common shocks and simultaneous failures. The same observation scheme, likelihood construction, censoring design, and performance criteria are used across models. Model performance is evaluated through Monte Carlo simulation using bias, integrated mean squared error, and empirical coverage, and the workflow is illustrated with the Device G reliability data. The results show that ignoring dependence can distort joint survival estimates, especially under moderate or high censoring. They also show that copula, frailty, and Marshall–Olkin specifications can lead to different reliability assessments because they encode different stochastic mechanisms. The estimation workflow includes multi-start optimization and diagnostics for boundary solutions, Hessian stability, and irregular likelihood behavior.

Keywords: joint survival analysis; competing risks; copula models; gamma frailty; reliability modeling; dependent failure modes

Check for updates

Received: 17 April 2026
Revised: 24 June 2026
Accepted: 30 June 2026
Published: 2 July 2026

Copyright: © 2026 by the authors. Licensee MDPI, Basel, Switzerland. This article is an open access article distributed under the terms and conditions of the Creative Commons Attribution (CC BY) license.

1. Introduction

The statistical problem considered in this article is the estimation and comparison of joint survival models for a population of comparable systems, devices, or individuals that may fail through two competing modes. From an independent sample of n measurements, the aim is to estimate the joint survival function

$$S(t_1, t_2) = \Pr\{T^{(1)} > t_1, T^{(2)} > t_2\},$$

and to assess how that estimate changes when dependence is modeled by independence, copulas, shared frailty, or Marshall–Olkin common shocks [1]. The paper is therefore an estimation and model-comparison study; it does not formulate a formal null-versus-alternative hypothesis test, and it does not introduce a new probability family.

A measurement may correspond, for example, to a field device observed until surge or wearout, a mechanical assembly exposed to component-specific and external shocks, or a patient followed until one of two causes terminates follow-up. These examples share the same statistical structure: two latent failure times compete, and the analyst observes only the first relevant event time or a censoring time. In a two-mode setting, let $T^{(1)}$ and $T^{(2)}$ denote the latent failure times for modes 1 and 2. The uncensored system failure time is

$$T = \min\{T^{(1)}, T^{(2)}\},$$

which is the standard representation used in lifetime-data and competing-risks models [2,3].

Under right censoring, the latent failure times are not observed directly. For each measurement, the record consists of the time at which follow-up ends and an event outcome indicating right censoring, failure by mode 1, failure by mode 2, or simultaneous failure. The formal observed-data notation is given in Section 2.1, where the recorded time and the four possible event outcomes are defined for the likelihood construction.

The marginal survival functions $S_1(t)$ and $S_2(t)$ are not sufficient to determine $S(t_1, t_2)$ unless independence is assumed. Under independence,

$$S(t_1, t_2) = S_1(t_1)S_2(t_2),$$

but shared operating conditions, manufacturing variability, material defects, or external shocks may induce dependence between the latent failure times. When such dependence is present, ignoring it can distort joint reliability estimates, especially under censoring [4,5].

Three established dependence mechanisms are compared in the same observed-data framework. In a survival copula model,

$$S_C(t_1, t_2) = C_\theta\{S_1(t_1), S_2(t_2)\},$$

where C_θ is a copula with dependence parameter θ [6,7]. In a shared frailty model, a positive latent variable Z acts on both cumulative hazards, giving the representation

$$S_F(t_1, t_2) = \mathbb{E}_Z[\exp\{-Z[H_1(t_1) + H_2(t_2)]\}],$$

which attributes association to unobserved measurement-level heterogeneity [8,9]. In a Marshall–Olkin model,

$$S_{MO}(t_1, t_2) = \exp\{-\Lambda_1(t_1) - \Lambda_2(t_2) - \Lambda_0[\max(t_1, t_2)]\},$$

and the common-shock component can place positive probability on the diagonal $t_1 = t_2$ [10–12].

These mechanisms answer different scientific questions. Copulas describe continuous association between marginal lifetimes, frailty models represent latent heterogeneity among measurements, and Marshall–Olkin models encode structural dependence caused by common shocks. The contribution of this article is to compare these mechanisms under the same observation scheme, likelihood construction, censoring design, simulation grid, and Device G illustration, rather than changing several elements of the analysis at once [13–15].

The independent Weibull model is used only as an algebraic benchmark. It provides the simplest sample likelihood and establishes a reference case from which the dependent specifications can be introduced. This ordering separates the statistical problem, the marginal model, and the dependence mechanism before the methodology and numerical results are presented.

The remainder of the paper is organized as follows. Section 2 defines the observed sample, the marginal survival models, the independent Weibull benchmark, and the dependence structures used throughout the study. Section 3 describes the likelihood-based estimation procedure, censoring mechanisms, simulation design, and performance metrics. Section 4 presents the simulation and Device G results. Section 5 discusses interpretation, numerical stability, and model choice. Section 6 summarizes the conclusions and future work.

2. Background and Model Framework

This section establishes the notation and probabilistic structure used throughout the article. We begin by defining the observed sample and by separating the latent failure process from the censoring mechanism. We then introduce the marginal exponential and Weibull models and use the independent Weibull case as a benchmark for the sample likelihood. The remaining subsections develop the dependent specifications considered in the study: Marshall–Olkin common shocks, copula-based association, and shared frailty.

2.1. Marginal Survival Models and Notation

Let $j = 1, \ldots, n$ index independent measurements from the population under study, and let $i \in \{1, 2\}$ index the two failure modes. A measurement may correspond to a device, a component assembly, or an individual under follow-up. For the j-th measurement, $T_j^{(1)}$ and $T_j^{(2)}$ denote the latent failure times associated with modes 1 and 2, and C_j denotes the right-censoring time. These are positive random variables on a common probability space. Under random censoring, C_j is independent of the latent failure process $(T_j^{(1)}, T_j^{(2)})$.

The observed sample is

$$\mathcal{D}_n = \{(Y_j, V_j) : j = 1, \ldots, n\}, \qquad Y_j = \min\{T_j^{(1)}, T_j^{(2)}, C_j\}, \tag{1}$$

where $V_j = (V_{1j}, V_{2j})$ is an event vertex taking values in

$$\mathcal{V} = \{(0,0), (1,0), (0,1), (1,1)\}. \tag{2}$$

The vertex is assigned by

$$V_j = \begin{cases} (0,0), & C_j < T_j^{(1)} \text{ and } C_j < T_j^{(2)}, \quad \text{right censored}, \\ (1,0), & T_j^{(1)} < T_j^{(2)} \text{ and } T_j^{(1)} \le C_j, \quad \text{failure by mode 1}, \\ (0,1), & T_j^{(2)} < T_j^{(1)} \text{ and } T_j^{(2)} \le C_j, \quad \text{failure by mode 2}, \\ (1,1), & T_j^{(1)} = T_j^{(2)} \le C_j, \quad \text{simultaneous failure}. \end{cases} \tag{3}$$

Thus, the sample element is the recorded time together with a point of the square $\{0,1\}^2$. The vertex $(1,1)$ has positive probability only when the joint law of $(T_j^{(1)}, T_j^{(2)})$ contains a singular component on the diagonal $t_1 = t_2$, as in Marshall–Olkin common-shock models [10,16]. In independent, copula, and frailty models with continuous margins, $\Pr\{V_j = (1,1)\} = 0$.

For a generic measurement, write $T^{(i)}$ for the marginal lifetime associated with failure mode i. Let

$$F_i(t) = \Pr\{T^{(i)} \le t\}, \qquad S_i(t) = 1 - F_i(t), \qquad f_i(t) = F_i'(t), \qquad h_i(t) = \frac{f_i(t)}{S_i(t)}.$$

Parametric marginal distributions, including exponential and Weibull models, are standard in lifetime data analysis and reliability engineering because they provide interpretable hazard shapes and closed-form survival functions [1,2,17]. In this article, the Weibull margin is written in rate form. We write $T^{(i)} \sim \text{Weibull}_r(\beta_i, \lambda_i)$ when $\beta_i > 0$ is the shape parameter and $\lambda_i > 0$ is the rate parameter. Then

$$F_i(t) = 1 - \exp(-\lambda_i t^{\beta_i}), \qquad t > 0, \tag{4}$$

and

$$S_i(t) = \exp(-\lambda_i t^{\beta_i}), \qquad f_i(t) = \lambda_i \beta_i t^{\beta_i - 1} \exp(-\lambda_i t^{\beta_i}). \tag{5}$$

If η_i denotes the usual Weibull scale parameter, then $\lambda_i = \eta_i^{-\beta_i}$ and

$$h_i(t) = \lambda_i \beta_i t^{\beta_i - 1}.$$

The shape parameter controls the hazard pattern: $\beta_i < 1$ gives a decreasing hazard, $\beta_i = 1$ gives the exponential case, and $\beta_i > 1$ gives an increasing hazard [17]. In several benchmark derivations below, a common shape parameter $\beta_1 = \beta_2 = \beta$ is used because it gives closed-form expressions and improves numerical stability under censoring [3].

The Weibull and exponential specifications used in this article have support on the positive half-line. Finite-support lifetime models, such as the Kies distribution and recent mixture extensions, may be useful when the physical observation window is bounded [18]. They are not fitted here because the objective is to compare dependence mechanisms under a common marginal framework.

Under non-informative censoring, factors involving only the censoring law are omitted from the likelihood. The likelihood of the sample is determined by the assumed joint law of $(T_j^{(1)}, T_j^{(2)})$. To introduce the notation without dependence parameters, we first write the independent Weibull benchmark. Suppose that the two latent risks have common shape $\beta > 0$ and cause-specific rates λ_1 and λ_2, so that

$$S(t_1, t_2) = S_1(t_1) S_2(t_2) = \exp(-\lambda_1 t_1^{\beta} - \lambda_2 t_2^{\beta}). \tag{6}$$

Under this continuous independent model, $\Pr\{V_j = (1,1)\} = 0$.

Let

$$r_1 = \sum_{j=1}^{n} \mathbf{1}\{V_j = (1,0)\}, \qquad r_2 = \sum_{j=1}^{n} \mathbf{1}\{V_j = (0,1)\}, \qquad m = r_1 + r_2.$$

The likelihood of the observed sample is

$$L(\beta, \lambda_1, \lambda_2; \mathcal{D}_n) = \prod_{j=1}^{n} \Big[\big(\lambda_1 \beta Y_j^{\beta-1}\big)^{\mathbf{1}\{V_j=(1,0)\}} \big(\lambda_2 \beta Y_j^{\beta-1}\big)^{\mathbf{1}\{V_j=(0,1)\}} \exp\{-(\lambda_1 + \lambda_2) Y_j^{\beta}\} \Big]. \tag{7}$$

The exponential factor is present for every measurement. The density factor for mode 1 appears only for $V_j = (1,0)$, and the density factor for mode 2 appears only for $V_j = (0,1)$. A censored measurement, $V_j = (0,0)$, therefore contributes only through the survival factor.

The log-likelihood, up to additive constants that do not involve the parameters, is

$$\ell(\beta, \lambda_1, \lambda_2; \mathcal{D}_n) = m \log \beta + r_1 \log \lambda_1 + r_2 \log \lambda_2 + (\beta - 1) \sum_{j:\, V_j \in \{(1,0),(0,1)\}} \log Y_j - (\lambda_1 + \lambda_2) \sum_{j=1}^{n} Y_j^{\beta}. \tag{8}$$

For fixed β, the profile estimators of the cause-specific rates are

$$\widehat{\lambda}_i(\beta) = \frac{r_i}{\sum_{j=1}^{n} Y_j^{\beta}}, \qquad i = 1, 2, \tag{9}$$

provided that $r_i > 0$. Substituting these estimators into the profile likelihood gives

$$\frac{m}{\beta} + \sum_{j:\, V_j \in \{(1,0),(0,1)\}} \log Y_j - m \frac{\sum_{j=1}^{n} Y_j^{\beta} \log Y_j}{\sum_{j=1}^{n} Y_j^{\beta}} = 0. \tag{10}$$

Equation (10) has no closed-form solution in general and is solved numerically over $\beta > 0$.

The maximum likelihood estimates are interpreted under the usual regularity conditions for parametric survival models: identifiable parameters, interior solutions, nondegenerate observed times, positive numbers of failures for estimable causes, differentiability of the log-likelihood, and a nonsingular information matrix [19]. These conditions can fail under heavy censoring, zero observed failures in one cause, boundary dependence parameters, or singular Marshall–Olkin components. For that reason, the numerical analyses report convergence diagnostics, Hessian checks, sensitivity to starting values, and profile-based uncertainty assessments when asymptotic normality is questionable.

2.2. Competing Risks and Minimum Failure Time

Using the observation scheme introduced in Section 2.1, this subsection outlines the distributional consequences of taking the minimum of two latent failure times. These analytical results provide algebraic benchmarks for the simulation study and for validating the likelihood implementation. Crucially, they are not used to impose independence in the dependent models considered later in this paper.

Let $T = \min\{T^{(1)}, T^{(2)}\}$ denote the uncensored system failure time. In competing risks and series-system settings, T represents the first latent failure time to occur, and an associated event vertex identifies the corresponding failure mode [3,10]. Under independence, the joint survival function factorizes as

$$S(t_1, t_2) = S_1(t_1) S_2(t_2),$$

whereby the survival function of the minimum simplifies to

$$\Pr(T > t) = \Pr\{T^{(1)} > t, T^{(2)} > t\} = S_1(t) S_2(t).$$

If $T^{(i)} \sim \text{Weibull}_r(\beta, \lambda_i)$ under the rate parametrization introduced in Section 2.1, then

$$\Pr(T > t) = \Pr\{T^{(1)} > t, T^{(2)} > t\} = \exp\{-(\lambda_1 + \lambda_2) t^{\beta}\},$$

and therefore

$$T \sim \text{Weibull}_r(\beta, \lambda_1 + \lambda_2).$$

This is the standard minimum distribution for two independent Weibull competing risks with a common shape parameter [20]. Equivalently, under the scale parametrization $\eta_i = \lambda_i^{-1/\beta}$, the scale parameter of T is

$$\eta_T = (\lambda_1 + \lambda_2)^{-1/\beta} = \left(\eta_1^{-\beta} + \eta_2^{-\beta}\right)^{-1/\beta}.$$

The exponential case arises as a special setting by fixing $\beta = 1$. Specifically, if $T^{(1)} \sim \text{Exp}(\lambda_1)$ and $T^{(2)} \sim \text{Exp}(\lambda_2)$ are independent, then

$$T = \min\{T^{(1)}, T^{(2)}\} \sim \text{Exp}(\lambda_1 + \lambda_2).$$

While this benchmark is useful for validating the independent baseline, such a factorization no longer holds when the failure times are dependent. In those settings, the distribution of the minimum must be explicitly derived from the selected joint survival model [6,21].

2.3. Structural Dependence via Marshall–Olkin Models

The independent Weibull benchmark introduced above has an absolutely continuous joint distribution and therefore satisfies $\Pr\{V_j = (1,1)\} = 0$. Marshall–Olkin models represent the complementary case in which a shared shock can produce $T_j^{(1)} = T_j^{(2)}$ with positive probability. Thus, this model class gives a direct probabilistic interpretation to the vertex $(1,1)$ in the observed sample.

For a generic measurement, let U_0 be a common shock time, and let U_1 and U_2 be mode-specific shock times. The latent failure times are

$$T^{(1)} = \min(U_1, U_0), \qquad T^{(2)} = \min(U_2, U_0). \tag{11}$$

If the common shock U_0 occurs before both mode-specific shocks and before censoring, then the observed vertex is $V = (1,1)$. This shock representation is the standard construction behind Marshall–Olkin dependence models in reliability and survival analysis [22].

For exponential shocks, assume that $U_k \sim \text{Exp}(\lambda_k)$, $k = 0,1,2$, are mutually independent, with $\lambda_k > 0$. Then

$$S_{\text{MOE}}(t_1, t_2) = \Pr\{T^{(1)} > t_1, T^{(2)} > t_2\} = \exp\{-\lambda_1 t_1 - \lambda_2 t_2 - \lambda_0 \max(t_1, t_2)\}. \tag{12}$$

Equation (12) is the bivariate specialization of the Marshall–Olkin multivariate exponential construction [10,23]. Here λ_0 is the common-shock intensity. When $\lambda_0 = 0$, the model reduces to independent exponential risks. When $\lambda_0 > 0$, the distribution has a singular component on the diagonal $t_1 = t_2$, and the probability of simultaneous failures is positive [21,24].

The Weibull extension used in this article keeps a common shape parameter $\beta > 0$ and writes the shock survival functions in rate form,

$$\Pr(U_k > t) = \exp(-\lambda_k t^\beta), \qquad k = 0,1,2.$$

The resulting Marshall–Olkin Weibull survival function is

$$S_{\text{MOW}}(t_1, t_2) = \exp\{-\lambda_1 t_1^\beta - \lambda_2 t_2^\beta - \lambda_0 \max(t_1, t_2)^\beta\}. \tag{13}$$

Equation (13) preserves the common-shock structure of the exponential model while replacing linear cumulative hazards by Weibull cumulative hazards. The rate parametrization keeps the additive structure on the cumulative-hazard scale, which is the natural scale for the Marshall–Olkin construction [16].

The marginal survival functions are

$$S_{T^{(1)}}(t) = \exp[-(\lambda_1 + \lambda_0)t^\beta], \qquad S_{T^{(2)}}(t) = \exp[-(\lambda_2 + \lambda_0)t^\beta], \tag{14}$$

and the uncensored system minimum satisfies

$$\Pr\{\min(T^{(1)}, T^{(2)}) > t\} = \exp[-(\lambda_0 + \lambda_1 + \lambda_2)t^{\beta}]. \tag{15}$$

Consequently,

$$\Pr\{T^{(1)} = T^{(2)}\} = \frac{\lambda_0}{\lambda_0 + \lambda_1 + \lambda_2}.$$

The diagonal component has one-dimensional density

$$g_0(t) = \lambda_0 \beta t^{\beta-1} \exp[-(\lambda_0 + \lambda_1 + \lambda_2)t^{\beta}], \qquad t > 0. \tag{16}$$

Equations (13)–(16) show that Marshall–Olkin models combine off-diagonal density terms, a one-dimensional diagonal term for simultaneous failures, and survival terms for censoring [10,16].

2.4. Likelihood-Based Inference Under Censoring

Using the observed-data notation introduced in Section 2.1, likelihood inference is based on the measurements (Y_j, V_j) rather than on the unobserved latent pair $(T_j^{(1)}, T_j^{(2)})$. Right censoring is treated as non-informative, so factors involving only the censoring distribution are omitted from the likelihood [1]. Let

$$S(t_1, t_2; \boldsymbol{\theta}) = \Pr_{\boldsymbol{\theta}}\{T^{(1)} > t_1, T^{(2)} > t_2\}$$

be the model-specific joint survival function.

The cause-specific subdensities are

$$g_1(y; \boldsymbol{\theta}) = \lim_{\varepsilon \downarrow 0} \left[-\frac{\partial}{\partial t_1} S(t_1, t_2; \boldsymbol{\theta}) \right]_{t_1 = y,\, t_2 = y+\varepsilon}, \qquad g_2(y; \boldsymbol{\theta}) = \lim_{\varepsilon \downarrow 0} \left[-\frac{\partial}{\partial t_2} S(t_1, t_2; \boldsymbol{\theta}) \right]_{t_1 = y+\varepsilon,\, t_2 = y}. \tag{17}$$

The one-sided notation is needed only when the joint survival function is not smooth on the diagonal, as in Marshall–Olkin models. If a singular diagonal component exists, simultaneous failures have one-dimensional density

$$g_0(y; \boldsymbol{\theta}) = \frac{d}{dy} \Pr_{\boldsymbol{\theta}}\{T^{(1)} = T^{(2)} \le y\}. \tag{18}$$

For independent, copula, and frailty models with continuous margins, this term is absent.

The likelihood of the sample is the product of four possible factors, selected by the vertex V_j:

$$L(\boldsymbol{\theta}; \mathcal{D}_n) = \prod_{j=1}^{n} [g_0(Y_j; \boldsymbol{\theta})]^{\mathbf{1}\{V_j=(1,1)\}} [g_1(Y_j; \boldsymbol{\theta})]^{\mathbf{1}\{V_j=(1,0)\}} [g_2(Y_j; \boldsymbol{\theta})]^{\mathbf{1}\{V_j=(0,1)\}} [S(Y_j, Y_j; \boldsymbol{\theta})]^{\mathbf{1}\{V_j=(0,0)\}}. \tag{19}$$

The four factors correspond to simultaneous failure, failure by mode 1, failure by mode 2, and right censoring. Copula and frailty models modify S, g_1, and g_2, whereas Marshall–Olkin models also retain g_0.

After maximizing $\ell(\boldsymbol{\theta}; \mathcal{D}_n) = \log L(\boldsymbol{\theta}; \mathcal{D}_n)$, the asymptotic variance–covariance matrix is estimated from the inverse observed information matrix,

$$\widehat{\mathrm{Var}}(\widehat{\boldsymbol{\theta}}) = \mathcal{I}_{\mathrm{obs}}(\widehat{\boldsymbol{\theta}})^{-1}, \qquad \mathcal{I}_{\mathrm{obs}}(\widehat{\boldsymbol{\theta}}) = -\left. \frac{\partial^2 \ell(\boldsymbol{\theta}; \mathcal{D}_n)}{\partial \boldsymbol{\theta}\, \partial \boldsymbol{\theta}^{\top}} \right|_{\boldsymbol{\theta} = \widehat{\boldsymbol{\theta}}}. \tag{20}$$

This approximation is used only when the Hessian is well conditioned and the regularity assumptions are plausible. If the Hessian is nearly singular, if the optimizer reaches a

boundary, or if simultaneous failures create nonregular behavior, confidence intervals are supplemented with profile likelihood or parametric bootstrap intervals [19,25,26].

2.5. Marshall–Olkin Weibull Likelihood Components

Section 2.3 defined the Marshall–Olkin Weibull survival function. We now collect the density and subdensity terms needed for the observed-data likelihood. To keep the notation light, the formulas are written for a generic measurement, with X_1 and X_2 used as generic versions of $T_j^{(1)}$ and $T_j^{(2)}$.

We use a rate parametrization for the Weibull distribution. Thus, $W \sim \text{Weibull}_r(\beta, \lambda)$ means

$$\Pr(W > w) = \exp(-\lambda w^\beta), \qquad w > 0,$$

where $\beta > 0$ is the shape parameter and $\lambda > 0$ is a rate parameter. The corresponding scale parameter is $\eta = \lambda^{-1/\beta}$. This convention avoids adding scale parameters directly and is better aligned with the Marshall–Olkin construction, where shock intensities add on the cumulative hazard scale. The same common-shape setting is used in the maximum likelihood development for Marshall–Olkin Weibull models [26].

Let U_0, U_1, and U_2 be mutually independent shock times with

$$\Pr(U_k > u) = \exp(-\lambda_k u^\beta), \qquad u > 0, \quad k = 0, 1, 2. \tag{21}$$

Here U_0 is the common-shock time, whereas U_1 and U_2 are mode-specific shock times. The latent failure times are

$$X_1 = \min(U_1, U_0), \qquad X_2 = \min(U_2, U_0). \tag{22}$$

The pair (X_1, X_2) follows a Marshall–Olkin Weibull model, denoted by

$$(X_1, X_2) \sim \text{MOW}(\beta, \lambda_0, \lambda_1, \lambda_2).$$

The parameter λ_0 represents the common-shock rate; if the common shock occurs first, both components fail at the same time, generating the singular diagonal event described by Marshall and Olkin [10].

With $z = \max(x_1, x_2)$, the joint survival function is

$$S_{X_1,X_2}(x_1, x_2) = \Pr(X_1 > x_1, X_2 > x_2) = \exp[-\lambda_1 x_1^\beta - \lambda_2 x_2^\beta - \lambda_0 z^\beta]. \tag{23}$$

Consequently, the marginal survival functions are

$$S_{X_1}(x) = \exp[-(\lambda_1 + \lambda_0)x^\beta], \qquad S_{X_2}(x) = \exp[-(\lambda_2 + \lambda_0)x^\beta]. \tag{24}$$

Equivalently,

$$X_1 \sim \text{Weibull}_r(\beta, \lambda_1 + \lambda_0), \qquad X_2 \sim \text{Weibull}_r(\beta, \lambda_2 + \lambda_0).$$

This expression should be interpreted in rate form: the quantities $\lambda_1 + \lambda_0$ and $\lambda_2 + \lambda_0$ are cumulative-hazard coefficients, not scale parameters.

The distribution of (X_1, X_2) is mixed. It has two absolutely continuous off-diagonal components and one singular component on the diagonal. For $x_1 < x_2$ and $x_2 < x_1$, the off-diagonal densities are

$$f_1(x_1, x_2) = \beta^2 \lambda_1 (\lambda_0 + \lambda_2) x_1^{\beta-1} x_2^{\beta-1} \exp[-\lambda_1 x_1^\beta - (\lambda_0 + \lambda_2) x_2^\beta], \tag{25}$$

$$f_2(x_1, x_2) = \beta^2 (\lambda_0 + \lambda_1) \lambda_2 x_1^{\beta-1} x_2^{\beta-1} \exp[-(\lambda_0 + \lambda_1) x_1^\beta - \lambda_2 x_2^\beta]. \tag{26}$$

The singular density on the diagonal, with respect to one-dimensional Lebesgue measure, is

$$f_0(x) = \beta \lambda_0 x^{\beta-1} \exp[-(\lambda_0 + \lambda_1 + \lambda_2) x^\beta], \qquad x > 0. \tag{27}$$

Thus, f_0 should not be interpreted as a two-dimensional density. It is the diagonal term associated with simultaneous failures. For the observed competing-risks likelihood, it is useful to define

$$\Lambda = \lambda_0 + \lambda_1 + \lambda_2.$$

The subdensities appearing in the generic likelihood (19) are then

$$g_0(y) = \beta \lambda_0 y^{\beta-1} e^{-\Lambda y^\beta}, \qquad g_1(y) = \beta \lambda_1 y^{\beta-1} e^{-\Lambda y^\beta}, \qquad g_2(y) = \beta \lambda_2 y^{\beta-1} e^{-\Lambda y^\beta}. \tag{28}$$

Here g_0 corresponds to simultaneous failure, g_1 to failure by mode 1, and g_2 to failure by mode 2. A censored observation at time y contributes through

$$S_{X_1,X_2}(y, y) = \exp(-\Lambda y^\beta). \tag{29}$$

When $\lambda_0 = 0$, the singular component disappears and the model reduces to independent Weibull risks with common shape β. When $\beta = 1$, the model reduces to the Marshall–Olkin exponential case. The expressions (28) and (29) are the quantities used in the maximum likelihood estimators presented in the following subsection.

2.6. Maximum Likelihood Estimators

We now specialize the sample likelihood to the Marshall–Olkin Weibull model. Let

$$m_{ab} = \sum_{j=1}^{n} \mathbf{1}\{V_j = (a, b)\}, \qquad (a, b) \in \mathcal{V}, \qquad m = m_{10} + m_{01} + m_{11}, \tag{30}$$

where m is the total number of observed failures. Censored measurements are counted by m_{00} and enter the likelihood through the survival factor.

For

$$\boldsymbol{\theta} = (\beta, \lambda_0, \lambda_1, \lambda_2), \qquad \lambda_+ = \lambda_0 + \lambda_1 + \lambda_2,$$

the event-specific terms in the MOW model are

$$g_0(Y_j; \boldsymbol{\theta}) = \beta \lambda_0 Y_j^{\beta-1} e^{-\lambda_+ Y_j^\beta}, \quad g_1(Y_j; \boldsymbol{\theta}) = \beta \lambda_1 Y_j^{\beta-1} e^{-\lambda_+ Y_j^\beta}, \quad g_2(Y_j; \boldsymbol{\theta}) = \beta \lambda_2 Y_j^{\beta-1} e^{-\lambda_+ Y_j^\beta}, \tag{31}$$

and a censored measurement contributes $S(Y_j, Y_j; \boldsymbol{\theta}) = \exp(-\lambda_+ Y_j^\beta)$. Hence the sample likelihood is

$$L(\boldsymbol{\theta}; \mathcal{D}_n) = \prod_{j=1}^{n} \left[\beta \lambda_0 Y_j^{\beta-1}\right]^{\mathbf{1}\{V_j=(1,1)\}} \left[\beta \lambda_1 Y_j^{\beta-1}\right]^{\mathbf{1}\{V_j=(1,0)\}} \left[\beta \lambda_2 Y_j^{\beta-1}\right]^{\mathbf{1}\{V_j=(0,1)\}} \exp(-\lambda_+ Y_j^\beta). \tag{32}$$

The corresponding log-likelihood is

$$\ell(\boldsymbol{\theta}; \mathcal{D}_n) = m \log \beta + m_{11} \log \lambda_0 + m_{10} \log \lambda_1 + m_{01} \log \lambda_2 + (\beta - 1) \sum_{j:\, V_j \neq (0,0)} \log Y_j - \lambda_+ \sum_{j=1}^{n} Y_j^{\beta}. \tag{33}$$

For a fixed value of β, define $Q(\beta) = \sum_{j=1}^{n} Y_j^{\beta}$. Maximizing with respect to $\lambda_0, \lambda_1, \lambda_2$ gives

$$\widehat{\lambda}_0(\beta) = \frac{m_{11}}{Q(\beta)}, \qquad \widehat{\lambda}_1(\beta) = \frac{m_{10}}{Q(\beta)}, \qquad \widehat{\lambda}_2(\beta) = \frac{m_{01}}{Q(\beta)}, \tag{34}$$

provided the corresponding count is positive. If $m_{11} = 0$, the likelihood is maximized at the boundary $\widehat{\lambda}_0 = 0$ in the closed parameter space. This is the nonregular situation noted for Marshall–Olkin exponential models by [27] and later discussed in the Weibull setting by [26].

Let

$$A = \sum_{j:\, V_j \neq (0,0)} \log Y_j, \qquad B(\beta) = \sum_{j=1}^{n} Y_j^{\beta} \log Y_j.$$

The profile score is

$$s_p(\beta) = \frac{m}{\beta} + A - m \frac{B(\beta)}{Q(\beta)} = 0. \tag{35}$$

This equation is solved numerically over $\beta > 0$. A fixed-point iteration similar to the procedure used by [28] is

$$\beta^{(r+1)} = h(\beta^{(r)}), \qquad h(\beta) = \frac{m\, Q(\beta)}{m\, B(\beta) - A\, Q(\beta)}, \tag{36}$$

whenever the denominator is positive. The iteration stops when $|\beta^{(r+1)} - \beta^{(r)}| < \varepsilon$, and the final rate estimates are obtained from (34).

When failure causes are ignored, only $T_{\min} = \min(X_1, X_2)$ is used. Under the MOW construction,

$$\Pr(T_{\min} > y) = \exp[-(\lambda_0 + \lambda_1 + \lambda_2) y^{\beta}]. \tag{37}$$

Thus ignored-cause data identify the total rate λ_+ but not the three shock components separately. This agrees with approximate maximum likelihood approaches for Weibull competing risks when cause information is not used [26,29,30].

For completeness, if $W = \log T_{\min}$, then

$$f_W(w; \mu, \sigma) = \frac{1}{\sigma} \exp\left\{ \frac{w - \mu}{\sigma} - \exp\left(\frac{w - \mu}{\sigma} \right) \right\}, \qquad w \in \mathbb{R}, \tag{38}$$

where $\sigma = 1/\beta$ and $\mu = -\sigma \log \lambda_+$. This transformation is useful for obtaining starting values, but the likelihood in (32) is used whenever the event vertex V_j is available. The next subsection uses the same observed-data notation to introduce copula and shared-frailty alternatives. Those models modify the joint survival structure, whereas the observation scheme (Y_j, V_j) remains unchanged.

2.7. Dependence Modeling: Copulas and Shared Frailty

The Marshall–Olkin model introduces dependence through a common shock and can therefore assign positive probability to $T^{(1)} = T^{(2)}$. Copula and shared-frailty models represent a different class of dependence mechanisms. They modify the joint survival

function while keeping the margins continuous; consequently, they do not create a diagonal atom, and

$$\Pr\{V_j = (1,1)\} = 0$$

under these models. Thus, their sample likelihood uses the same terms for censoring and cause-specific failures as in Equation (19), but without the singular term g_0.

For a survival copula model, the joint survival function is written as

$$S_C(t_1, t_2; \boldsymbol{\theta}) = C_\theta\{S_1(t_1), S_2(t_2)\}, \tag{39}$$

where S_1 and S_2 are the selected marginal survival functions and C_θ is a copula with dependence parameter θ. This construction keeps marginal modeling separate from dependence modeling, which is one of the main reasons copulas are useful in reliability and survival analysis [6]. In this study, dependence strength is reported through Kendall's τ, because it provides a common scale for comparing the Gumbel and Clayton families [31].

2.7.1. Gumbel Copula

The Gumbel copula is defined by

$$C_G(u, v; \theta) = \exp\left\{-\left[(-\log u)^\theta + (-\log v)^\theta\right]^{1/\theta}\right\}, \qquad 0 < u, v < 1, \quad \theta \geq 1. \tag{40}$$

The case $\theta = 1$ gives independence, whereas $\theta > 1$ induces positive dependence. On the copula scale, the Gumbel family emphasizes upper-tail association and is therefore useful when strong joint survival or reliability behavior is expected in the upper tail [32]. Kendall's coefficient is

$$\tau_G = 1 - \frac{1}{\theta}, \qquad \theta = \frac{1}{1 - \tau_G}. \tag{41}$$

Because the margins are continuous, this model can represent strong association but not exact simultaneous failures.

2.7.2. Clayton Copula

The Clayton copula is given by

$$C_C(u, v; \theta) = \left(u^{-\theta} + v^{-\theta} - 1\right)^{-1/\theta}, \qquad 0 < u, v < 1, \quad \theta > 0. \tag{42}$$

This family emphasizes lower-tail association on the copula scale and is often used when dependence is expected to be stronger in one tail of the joint distribution [33]. Kendall's coefficient satisfies

$$\tau_C = \frac{\theta}{\theta + 2}, \qquad \theta = \frac{2\tau_C}{1 - \tau_C}. \tag{43}$$

As with the Gumbel copula, the Clayton model changes the joint survival structure but does not introduce a singular diagonal component when the margins are continuous.

2.7.3. Shared Frailty

Shared frailty models induce dependence through an unobserved measurement-level random effect. Conditional on a positive frailty variable $Z = z$, both cumulative hazards are multiplied by the same factor:

$$S_F(t_1, t_2 \mid Z = z) = \exp[-z\{H_1(t_1) + H_2(t_2)\}], \tag{44}$$

where $H_i(t) = -\log S_i(t)$ is the marginal cumulative hazard for mode i. This construction is useful when dependence is attributed to unmeasured manufacturing conditions, environmental exposure, or usage variability rather than to an exact common shock [22,34].

In the gamma frailty specification used here, $Z \sim \text{Gamma}(\alpha, \alpha)$ in the shape–rate parameterization, so that $\mathbb{E}(Z) = 1$ and $\text{Var}(Z) = 1/\alpha$. Integrating (44) over Z gives

$$S_F(t_1, t_2) = \left[1 + \frac{H_1(t_1) + H_2(t_2)}{\alpha}\right]^{-\alpha}. \tag{45}$$

Small values of α imply larger frailty variance and stronger positive association between the failure modes; as $\alpha \to \infty$, the model approaches independence. This interpretation follows the standard shared frailty framework for multivariate time-to-event data [8].

The three dependence mechanisms considered in this section therefore have different stochastic meanings. Copulas modify the association between the marginal survival functions, shared frailty introduces latent heterogeneity, and Marshall–Olkin models represent common shocks with a possible diagonal mass. Keeping these mechanisms separate is important for the simulation study, because the same observed-data scheme (Y_j, V_j) can lead to different joint survival estimates depending on how dependence is generated.

3. Methodology

This section describes the estimation, simulation, and evaluation procedures used to compare the dependence models introduced in Section 2. All models are fitted using the observed-data structure defined in Section 2.1, so differences in performance can be attributed to the assumed dependence mechanism rather than to a change in notation, censoring scheme, or estimation target. The methodology is organized around four steps: defining the censoring mechanism, constructing the observed-data likelihood, estimating the model parameters, and evaluating the estimated joint survival function.

3.1. Observation Scheme and Censoring Mechanism

The observation scheme follows Equations (1)–(3). For random censoring, C_j is generated independently of the latent failure process $(T_j^{(1)}, T_j^{(2)})$. If π_c denotes the target censoring proportion, the censoring distribution is calibrated so that

$$\Pr\{C_j < \min(T_j^{(1)}, T_j^{(2)})\} \approx \pi_c,$$

where the approximation is understood over Monte Carlo replications. For Type I censoring, $C_j \equiv C$ is fixed by design. The vertex $(1, 1)$ is generated only under Marshall–Olkin data-generating mechanisms, where a common shock can produce $T_j^{(1)} = T_j^{(2)}$ with positive probability.

3.2. Likelihood Construction Under Dependence

Let M denote a candidate model and let $S_M(t_1, t_2; \boldsymbol{\theta}_M)$ be its joint survival function. The parameter vector $\boldsymbol{\theta}_M$ contains the marginal parameters and, when applicable, the dependence parameter. For each observation type, define the model-specific terms

$$g_{1M}(y; \boldsymbol{\theta}_M), \qquad g_{2M}(y; \boldsymbol{\theta}_M), \qquad g_{0M}(y; \boldsymbol{\theta}_M),$$

where g_{1M} and g_{2M} are the cause-specific subdensities, and g_{0M} is the diagonal term when the model has a singular common-shock component. For independent, copula, and

frailty models with continuous margins, the term g_{0M} is omitted because $V_j = (1,1)$ has probability zero.

The observed-data likelihood factor is

$$L_{jM}(\boldsymbol{\theta}_M; Y_j, V_j) = [g_{0M}(Y_j; \boldsymbol{\theta}_M)]^{\mathbf{1}\{V_j=(1,1)\}} [g_{1M}(Y_j; \boldsymbol{\theta}_M)]^{\mathbf{1}\{V_j=(1,0)\}} [g_{2M}(Y_j; \boldsymbol{\theta}_M)]^{\mathbf{1}\{V_j=(0,1)\}} [S_M(Y_j, Y_j; \boldsymbol{\theta}_M)]^{\mathbf{1}\{V_j=(0,0)\}}, \quad (46)$$

with the first factor included only for models with a singular diagonal component. The sample likelihood and log-likelihood are

$$L_M(\boldsymbol{\theta}_M; \mathcal{D}_n) = \prod_{j=1}^{n} L_{jM}(\boldsymbol{\theta}_M; Y_j, V_j), \qquad \ell_M(\boldsymbol{\theta}_M; \mathcal{D}_n) = \sum_{j=1}^{n} \log L_{jM}(\boldsymbol{\theta}_M; Y_j, V_j). \quad (47)$$

This notation keeps the likelihood tied to the observed sample. Copula and frailty models modify S_M, g_{1M}, and g_{2M} through their dependence structure. Marshall–Olkin models also retain g_{0M}, which preserves the common-shock interpretation instead of treating simultaneous failures as ordinary continuous ties.

3.3. Parameter Estimation Procedure

Maximum likelihood estimates are computed numerically. Closed-form estimators are available only for a few benchmark cases, and the likelihood can become nearly flat, multimodal, or boundary constrained when censoring is heavy. To reduce sensitivity to local optima, each model is fitted from several starting values. Positive parameters are optimized on the logarithmic scale, and copula parameters are constrained to their natural domains. The reported estimate is the converged solution with the largest finite log-likelihood across the multi-start runs. This strategy follows standard practice for nonlinear likelihood optimization [35]. The complete estimation workflow is summarized in Algorithm 1.

Algorithm 1 Maximum Likelihood Estimation under Dependence

Require: Observed data $\mathcal{D}_n = \{(Y_j, V_j)\}_{j=1}^n$, candidate model M, parameter domain Θ_M, and tolerance ε.

Ensure: Estimate $\widehat{\boldsymbol{\theta}}_M$, maximized log-likelihood, convergence diagnostics, and variance–covariance matrix when regularity conditions are plausible.

1: Specify the marginal distributions and the dependence mechanism: independence, Archimedean copula, shared gamma frailty, MOE, or MOW.
2: Construct $S_M(t_1, t_2; \boldsymbol{\theta}_M)$ and the corresponding cause-specific, censoring, and, when needed, diagonal terms.
3: Build $\ell_M(\boldsymbol{\theta}_M; \mathcal{D}_n) = \sum_{j=1}^n \log L_{jM}(\boldsymbol{\theta}_M; Y_j, V_j)$ using the vertex $V_j \in \mathcal{V}$.
4: Generate starting values from marginal Weibull fits, moment-based approximations, profile likelihood values, and dispersed random perturbations.
5: Maximize $\ell_M(\boldsymbol{\theta}_M; \mathcal{D}_n)$ using bounded quasi-Newton optimization, or derivative-free optimization when derivatives are unstable.
6: Repeat the optimization over all starting values and retain the converged solution with the largest finite log-likelihood.
7: Check convergence codes, gradients, boundary solutions, Hessian eigenvalues, and profile likelihoods for key parameters.
8: Compute standard errors from the inverse observed information when it is positive definite; otherwise report profile likelihood or bootstrap intervals.

For reproducibility, the implementation records the software environment, package versions, starting values, convergence codes, number of iterations, and elapsed time for each fitted model. The analyses were implemented in R, using base optimization routines together with survival-analysis and copula utilities [36]. In the replication scripts, opti-

mization was stopped when the change in the log-likelihood was below 10^{-8} or when the change in the parameter vector was below 10^{-6}.

Computational cost was also recorded. Independence and marginal Weibull models are fast because they involve low-dimensional likelihoods. Copula and frailty models require repeated evaluation of the joint survival function or numerical integration. MOW models are more demanding because their likelihood combines continuous off-diagonal terms with the singular diagonal term. Reporting elapsed time by scenario makes the comparison more reproducible and allows the reader to assess the computational cost of each dependence mechanism.

Stability was assessed in three ways. First, each model was estimated from multiple starting points. Second, one-dimensional profile likelihoods were inspected for influential parameters, especially the Weibull shape and dependence parameters. Third, bootstrap resampling was used when the observed information matrix was ill conditioned or when profile likelihoods indicated noticeable asymmetry.

Under standard regularity conditions, maximum likelihood estimators are consistent and asymptotically normal [19]. These properties are used only when the fitted model is identifiable, the estimate lies in the interior of the parameter space, and the observed information matrix is nonsingular. When these conditions are doubtful, for example under heavy censoring, zero failures in one cause, or boundary dependence estimates, the results are reported as likelihood-based numerical estimates and uncertainty is summarized using profile likelihood or bootstrap intervals. Moment-based, probability-plot, and profile estimators are used as starting values and sensitivity checks. The sample likelihood remains the main estimation criterion because it incorporates censoring, event vertices, and simultaneous failures in a single observed-data formulation.

3.4. Simulation Design

A Monte Carlo simulation study was conducted to compare estimation accuracy under correct and misspecified dependence models. Let $\mathcal{G}$ denote the set of data-generating mechanisms and let $\mathcal{M}$ denote the set of candidate fitted models. The data-generating mechanisms include independent risks, Archimedean copulas, shared gamma frailty, and Marshall–Olkin common shocks. The candidate models are fitted to the same simulated datasets so that differences in performance reflect the fitted dependence structure.

Each simulation scenario is defined by

$$(n, \tau, \pi_c, G),$$

where n is the sample size, τ is the target dependence strength when Kendall's coefficient is applicable, π_c is the target censoring proportion, and $G \in \mathcal{G}$ is the data-generating mechanism. For Marshall–Olkin models, the common-shock rate is selected to produce the desired simultaneous failure probability or its closest feasible counterpart under the chosen parameterization. For copula and frailty mechanisms with continuous margins, simultaneous failures are not generated.

For each scenario, R independent datasets are generated. The same marginal parameters and censoring design are used across dependence mechanisms whenever possible. This keeps the simulation focused on the effect of dependence rather than on changes in marginal lifetime behavior. All computations were carried out in R [36]. The simulation and evaluation workflow is summarized in Algorithm 2.

Algorithm 2 Simulation and Evaluation Framework

Require: Scenario grid for n, dependence strength τ, censoring level π_c, data-generating mechanisms $\mathcal{G}$, fitted models $\mathcal{M}$, and number of replications R.
Ensure: Bias, IMSE, coverage probabilities, convergence summaries, and computational times.

```
for each data-generating mechanism G ∈ 𝒢 do
  for each sample size n do
    for each dependence level τ do
      for each censoring level π_c do
        for r = 1, ..., R do
          Generate latent failure times (T_j^(1), T_j^(2)), j = 1, ..., n, under mechanism G.
          Generate censoring times and construct (Y_j, V_j) using Equations (1)–(3).
          for each fitted model M ∈ ℳ do
            Estimate θ_M using Algorithm 1.
            Compute the estimated joint survival function Ŝ_rM(t_1, t_2) on the evaluation grid.
            Store convergence diagnostics, uncertainty intervals, and elapsed time.
          end for
        end for
      end for
    end for
  end for
end for
Aggregate performance metrics across replications.
```

3.5. Performance Metrics

Performance is evaluated primarily on the joint survival scale, because the main inferential target is

$$S(t_1, t_2) = \Pr\{T^{(1)} > t_1, T^{(2)} > t_2\}.$$

Let $\mathcal{T}$ be the grid of time pairs used to evaluate the joint survival function, and let $S_G(t_1, t_2)$ be the true joint survival function under the data-generating mechanism G. For replication r and fitted model M, denote the estimated joint survival function by $\widehat{S}_{rM}(t_1, t_2)$.

The pointwise bias of the estimated joint survival function is

$$\mathrm{Bias}_{M,G}(t_1, t_2) = \frac{1}{R} \sum_{r=1}^{R} \left\{ \widehat{S}_{rM}(t_1, t_2) - S_G(t_1, t_2) \right\}. \tag{48}$$

The integrated mean squared error is approximated over $\mathcal{T}$ by

$$\mathrm{IMSE}_{M,G} = \frac{1}{|\mathcal{T}|} \sum_{(t_1,t_2)\in\mathcal{T}} \frac{1}{R} \sum_{r=1}^{R} \left\{ \widehat{S}_{rM}(t_1, t_2) - S_G(t_1, t_2) \right\}^2. \tag{49}$$

When confidence bands or pointwise intervals are computed, empirical coverage is estimated as

$$\mathrm{Cov}_{M,G} = \frac{1}{|\mathcal{T}|} \sum_{(t_1,t_2)\in\mathcal{T}} \frac{1}{R} \sum_{r=1}^{R} \mathbf{1}[S_G(t_1, t_2) \in \mathcal{C}_{rM}(t_1, t_2)], \tag{50}$$

where $\mathcal{C}_{rM}(t_1, t_2)$ is the interval or band reported by model M in replication r.

Parameter bias is reported only for parameters that are identifiable and meaningfully comparable under the data-generating mechanism. For example, marginal Weibull parameters and Kendall's τ can be compared across some models, whereas the Marshall–Olkin common-shock rate and the frailty variance represent different stochastic mechanisms. For this reason, IMSE and coverage of $S(t_1, t_2)$ are the main criteria for comparing fitted models.

4. Results

This section reports the Monte Carlo comparison and the Device G application. The results are interpreted on the joint survival scale,

$$S(t_1, t_2) = \Pr\{T^{(1)} > t_1, T^{(2)} > t_2\},$$

because this quantity is directly affected by the assumed dependence mechanism. The simulation results first compare the fitted models under controlled censoring levels. The real-data analysis then illustrates how the same modeling choices change reliability assessment for a device with two competing failure modes. The R workflow used to reproduce the simulations is summarized in Appendix A.

4.1. Simulation Study for Marshall–Olkin Models and Comparative Approaches

The simulation study was designed to evaluate how well each fitted model recovers the joint survival function when the underlying dependence mechanism is known. The same observed-data structure defined in Section 2.1 was used for all fitted models. This keeps the focus on the dependence specification rather than on changes in the sample definition, censoring rule, or performance metric.

The fitted model set was

$$\mathcal{M} = \{\text{IndepW}, \text{GumbelW}, \text{ClaytonW}, \text{FrailtyW}, \text{MOE}, \text{MOW}\}.$$

Here IndepW denotes the independent Weibull benchmark, GumbelW and ClaytonW denote Weibull-margin copula models, FrailtyW denotes the shared gamma frailty model with Weibull margins, and MOE and MOW denote the Marshall–Olkin exponential and Weibull models, respectively.

For each scenario, $R = 1000$ Monte Carlo datasets were generated with sample sizes $n \in \{200, 500\}$ and censoring targets $c \in \{0\%, 10\%, 30\%, 50\%\}$. Weibull margins were generated in rate form,

$$S_i(t) = \exp(-\lambda_i t^{\alpha_i}),$$

with $(\alpha_1, \lambda_1) = (1.2, 1.0)$ for mode 1 and $(\alpha_2, \lambda_2) = (1.5, 0.8)$ for mode 2. Copula dependence was indexed by Kendall's $\tau \in \{0.2, 0.5\}$, using $\theta_{\text{Gumbel}} = (1-\tau)^{-1}$ and $\theta_{\text{Clayton}} = 2\tau/(1-\tau)$. The shared gamma frailty model used $Z \sim \text{Gamma}(2, 2)$, so that $\mathbb{E}(Z) = 1$ and $\text{Var}(Z) = 0.5$. For Marshall–Olkin scenarios, the common-shock component was chosen to produce a non-negligible diagonal term, so that simultaneous failures could be generated under MOE and MOW but not under the continuous copula or frailty models.

The data-generating mechanism followed the definitions in Section 2. Under independence, $T_j^{(1)}$ and $T_j^{(2)}$ were generated separately from their marginal distributions. Under copula dependence, (U_{1j}, U_{2j}) was generated from the selected Archimedean copula and then transformed through $T_j^{(i)} = F_i^{-1}(U_{ij})$. Under shared frailty, the measurement-specific frailty Z_j was generated first and the conditional hazards were multiplied by Z_j. Under MOE and MOW, individual and common shocks were generated independently and the latent failure times were set to

$$T_j^{(1)} = \min(U_{1j}, U_{0j}), \qquad T_j^{(2)} = \min(U_{2j}, U_{0j}).$$

Random censoring was then applied through $Y_j = \min(T_j^{(1)}, T_j^{(2)}, C_j)$, with C_j generated independently of the latent failure process. Model accuracy was evaluated on a grid

$$\mathcal{T} = \{(t_{1g}, t_{2g}) : g = 1, \ldots, G\}.$$

For replication r and fitted model M, let $\widehat{S}_r^{(M)}(t_{1g}, t_{2g})$ denote the estimated joint survival function, and let $S_0(t_{1g}, t_{2g})$ be the true joint survival function under the data-generating scenario. The integrated mean squared error was computed as

$$\mathrm{IMSE}(M) = \frac{1}{R}\sum_{r=1}^{R}\frac{1}{G}\sum_{g=1}^{G}\left\{\widehat{S}_r^{(M)}(t_{1g}, t_{2g}) - S_0(t_{1g}, t_{2g})\right\}^2. \tag{51}$$

Bias and empirical coverage of the Y_e confidence bands were computed on the same grid. Here, Y_e denotes the log–log survival transformation

$$Y_e(t_1, t_2) = \log[-\log\{\widehat{S}(t_1, t_2)\}],$$

which was used to construct bands before back-transforming them to the survival scale.

Figure 1 shows that all fitted models produce monotonically decreasing joint survival surfaces, but the contour patterns are different. The independent Weibull model has product-type contours, as expected from $S(t_1, t_2) = S_1(t_1)S_2(t_2)$. The Gumbel and Clayton copulas bend the contours in different parts of the grid, reflecting their upper- and lower-tail association patterns. The frailty model produces a smoother form of positive association because dependence is induced by a shared latent multiplier rather than by an explicit shock.

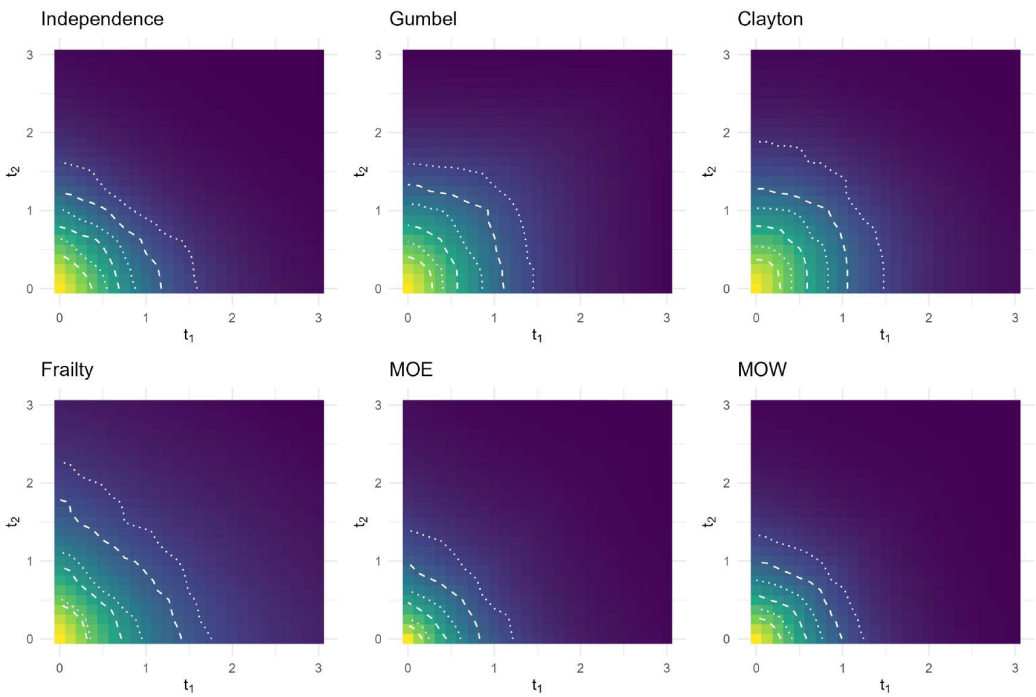

Figure 1. Joint survival surfaces and contour lines for the six fitted dependence specifications considered in the simulation study. The surfaces are compared on the same time grid to show how the dependence mechanism changes the geometry of $S(t_1, t_2)$.

The Marshall–Olkin surfaces show the clearest structural contrast. Their geometry reflects the common-shock mechanism, which can place probability mass on the diagonal $t_1 = t_2$. This feature is especially visible in the middle region of the grid, where models with similar marginal behavior can still give different estimates of joint reliability. The figure therefore provides a visual check of the main premise of the comparison: dependence models that look similar at the marginal level can lead to different joint survival assessments.

Table 1 reports the IMSE values for the six fitted models across the four censoring levels. The MOW model gives the smallest error under 0%, 10%, and 30% censoring. This

is consistent with the simulation design, because the Marshall–Olkin Weibull model can reproduce both the Weibull margins and the common-shock structure. The MOE model is also competitive at low censoring, but its error increases when the Weibull shape is needed to capture the time-varying failure behavior.

Table 1. Integrated mean squared error (IMSE) for joint survival estimation across censoring levels. Smaller values indicate closer agreement with the true joint survival surface on the evaluation grid.

Model	0%	10%	30%	50%
IndepW	0.1668890	0.2104161	0.3494275	0.8715601
GumbelW	1.9851585	2.0473139	2.2272948	3.0657810
ClaytonW	1.4321967	1.5218191	1.5725923	2.2767248
FrailtyW	8.5135595	8.9118002	9.1411798	9.3839502
MOE	0.1603779	0.1835660	0.3789848	1.1472263
MOW	0.1347112	0.1733760	0.3001097	0.9223216

The independent Weibull model is close to the Marshall–Olkin models when the data are complete or only lightly censored. At 50% censoring, it has the smallest numerical IMSE in the table, although the difference from MOW is small relative to the deterioration caused by censoring. This result should not be read as evidence that independence is generally preferable. Rather, it shows that heavy censoring can reduce the information available to distinguish dependence mechanisms, especially when the comparison is made only through an aggregate error measure.

The copula models have intermediate errors in this simulation design. ClaytonW performs better than GumbelW across all censoring levels, but both are less accurate than the Marshall–Olkin models when the data-generating process contains a common-shock component. This is expected: copulas can represent smooth dependence between continuous margins, but they do not generate exact simultaneous failures. The frailty model has the largest IMSE values. This does not mean that shared frailty is generally unsuitable; it means that, in these scenarios, latent heterogeneity alone does not reproduce the structural common-shock behavior present in the data-generating mechanism.

Across the table, censoring increases the difficulty of joint survival estimation. For most models, IMSE grows as the censoring proportion rises. The increase is especially clear for the independent, copula, and MOE fits. This pattern is consistent with the methodological expectation that censoring affects not only marginal estimation but also the ability to recover the dependence structure. The practical implication is that model choice becomes more consequential when the available failure information is incomplete.

4.2. Application with Real Data: Device G Study

The Device G data described by [1] come from a field follow-up study with two failure modes. The first mode, surge, is associated with random electrical damage; the second mode, wearout, is associated with use-related degradation. The dataset is used here as an applied illustration of the proposed workflow. The purpose is not to claim that a single dependence model is the true data-generating mechanism for Device G, but to show how different assumptions change the estimated joint reliability when the same observed data are analyzed.

Weibull margins were fitted separately to the two modes. For the surge mode, the estimated shape parameter was $\beta = 1.490$ and the scale was $\eta = \exp(6.108)$. For the wearout mode, the estimated shape parameter was $\beta = 0.231$ and the scale was $\eta = \exp(5.830)$. Three joint survival estimators were then compared:

$$\widehat{S}_{\mathrm{Ind}}(t_1, t_2) = \widehat{S}_1(t_1)\widehat{S}_2(t_2),$$

a Gumbel copula estimator, and a Gumbel copula estimator combined with shared gamma frailty. The Gumbel copula was fitted with $\theta = 2$, and the shared gamma frailty was parameterized with mean 1 and variance $1/\alpha$, with α fixed according to the simulation setting used for the sensitivity analysis. To evaluate sensitivity to incomplete follow-up, random censoring levels of 0%, 10%, 30%, and 50% were imposed.

Figure 2 compares the survival estimates obtained under different censoring levels. With complete data, the independent and Gumbel-based estimates remain close over much of the time range. This is reasonable because complete failure information reduces the ambiguity between dependence specifications. As censoring increases, the curves begin to separate earlier. Under 30% and 50% censoring, the independent estimate declines more quickly than the Gumbel-based estimate, indicating greater sensitivity to the loss of event-time information.

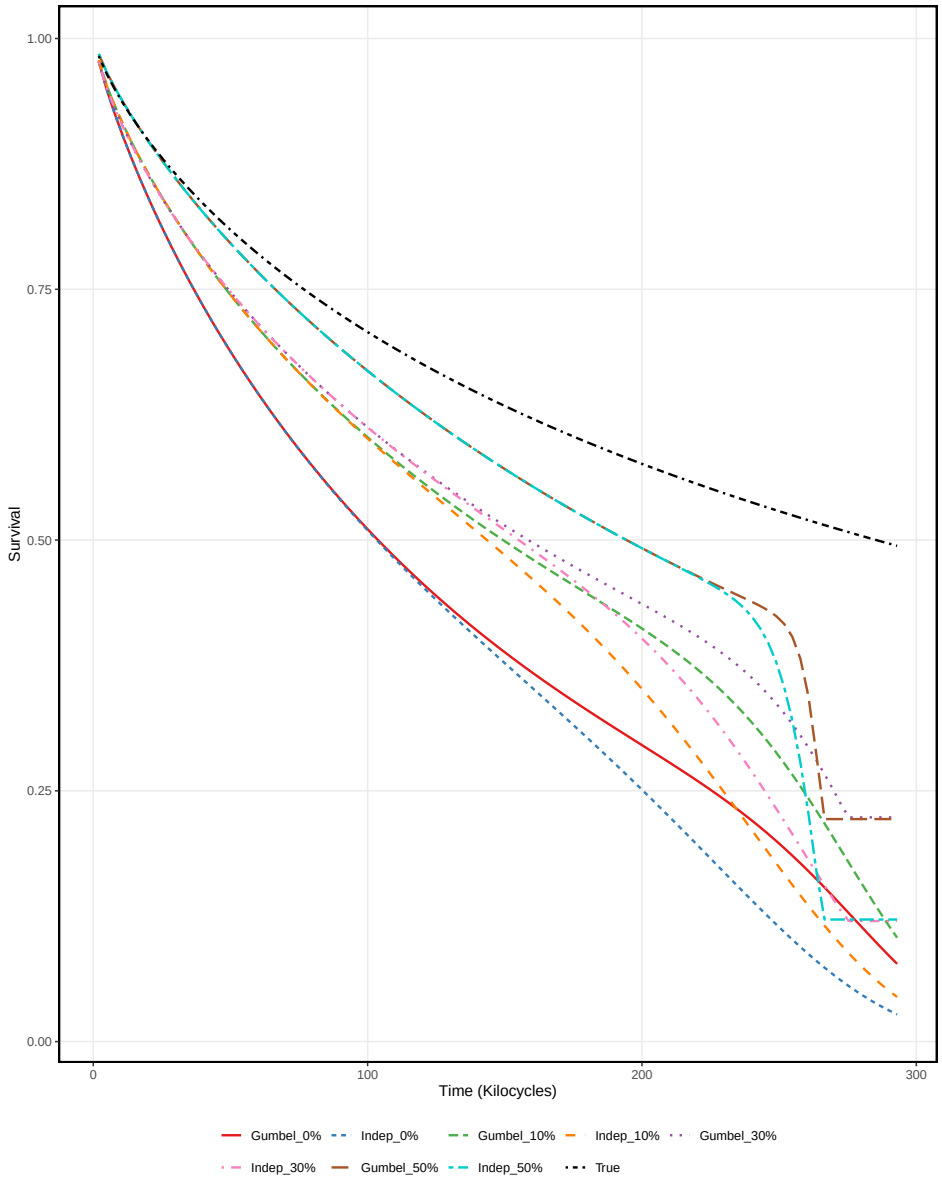

Figure 2. Estimated Device G survival curves under independence and Gumbel dependence across censoring levels, including the complete-data reference.

The 50% censoring case is the most informative for interpretation. In that setting, the independent estimate drops sharply in the later part of the time range, whereas the Gumbel

estimate remains closer to the complete-data reference. Both estimates become less stable under heavy censoring, but the dependent model preserves more of the survival pattern seen with fuller information. The main message is therefore not that the Gumbel model is always correct, but that dependence assumptions can become visible once the observed failure information is reduced.

Figure 3 focuses on the censored scenarios. At 10% censoring, the two model classes remain relatively close during the early part of follow-up. At 30% and 50% censoring, the gap widens. The dependent Gumbel estimates generally remain higher than the independent estimates at comparable time points. This pattern suggests that the independence assumption can lead to a more pessimistic estimate of joint reliability for Device G when the data are strongly censored.

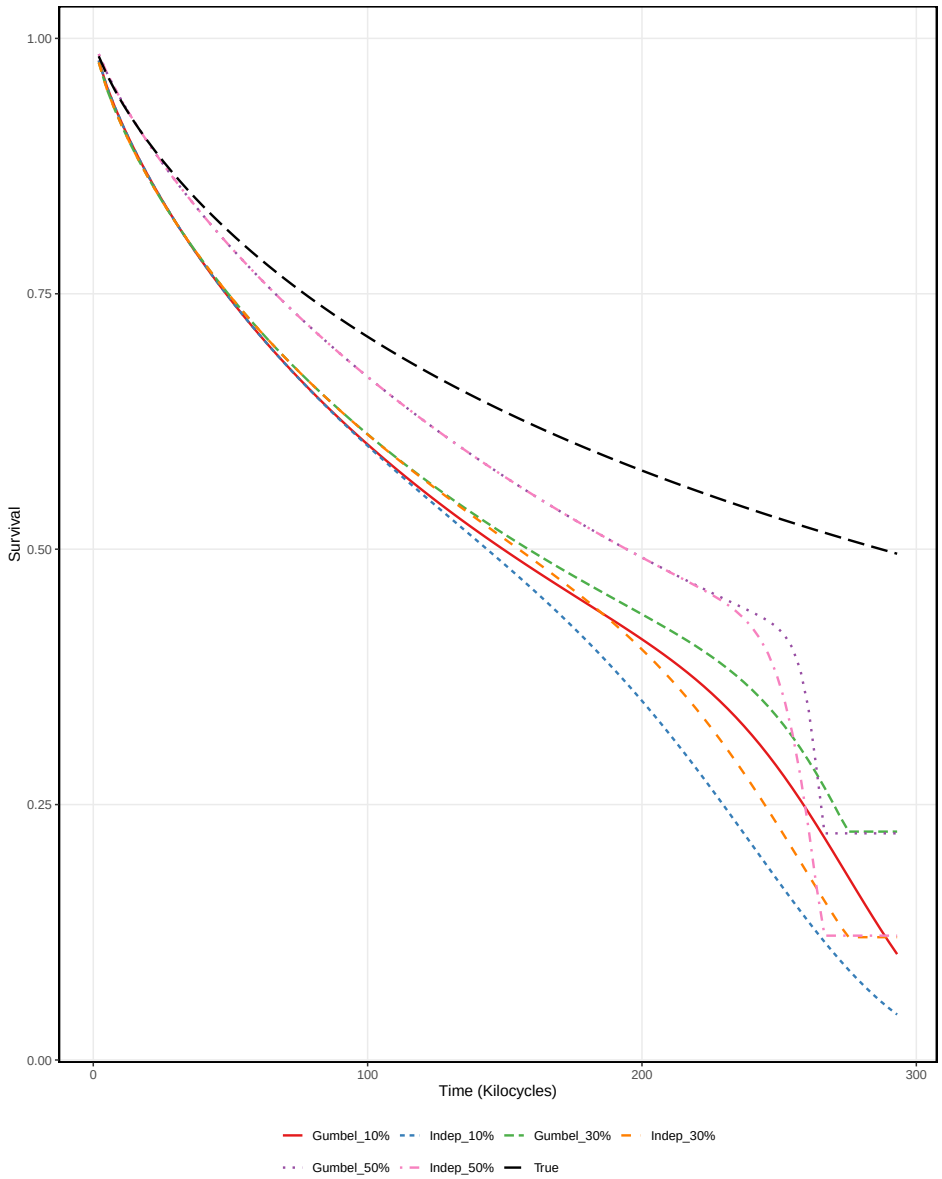

Figure 3. Estimated Device G survival curves under positive censoring levels. The plot removes the complete-data case to make the separation between independence and Gumbel dependence easier to inspect.

The figure also shows why the real-data analysis should be interpreted as a sensitivity study. The available Device G observations do not prove a unique dependence mechanism. They do show, however, that the joint reliability curve can change noticeably when depen-

dence between failure modes is modeled rather than suppressed. This is the practical issue that the simulation study was designed to examine under controlled conditions.

Figure 4 presents the Gumbel copula estimate with 95% confidence bands obtained through the Y_e procedure. The point estimate decreases smoothly over the observed time range, as expected for a survival function. The confidence bands are narrower where more observations remain informative and become wider in the tail, where fewer measurements contribute information. This widening is a feature of the data structure rather than a failure of the method: uncertainty necessarily increases when survival is estimated from a smaller effective risk set.

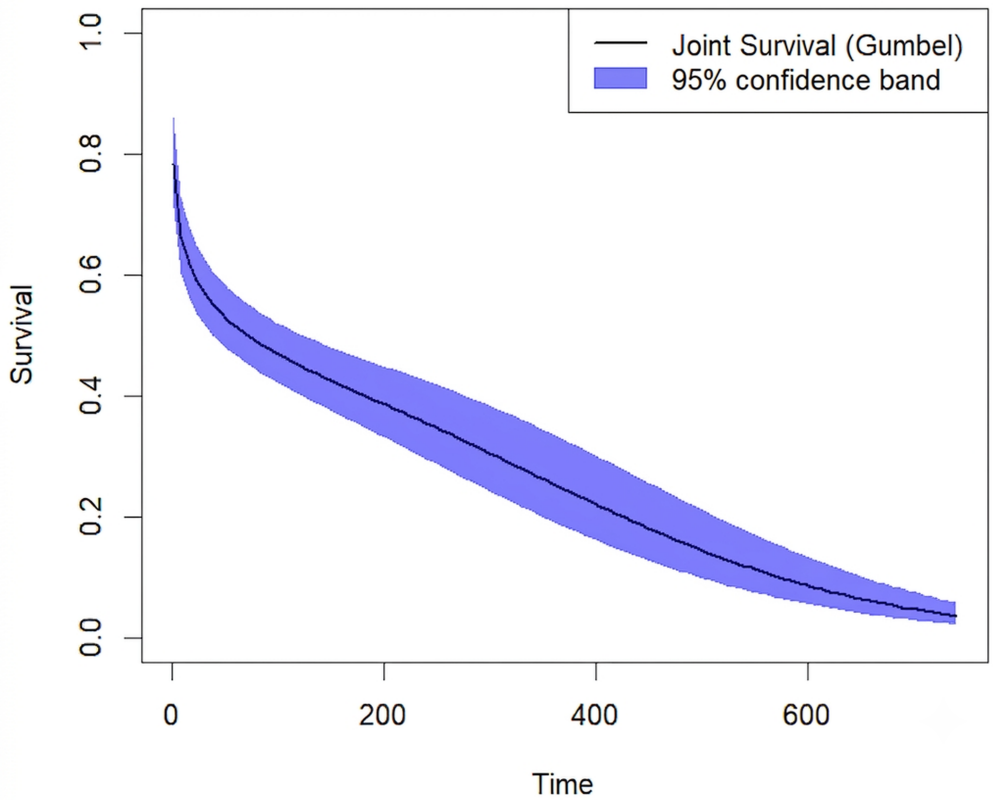

Figure 4. Gumbel copula estimate of the Device G joint survival function. Note: The black solid line represents the estimated joint survival curve. The purple shaded region represents the 95% confidence band obtained using the Y_e procedure and back-transformed to the survival scale.

The confidence bands also help separate two issues that are often conflated. The point estimate describes the fitted joint survival curve under the selected dependence model. The band describes uncertainty around that fitted curve. A narrow band would not prove that the Gumbel copula is the correct dependence mechanism, and a wider band does not invalidate the model. Rather, the band shows how much sampling uncertainty remains after the model has been chosen.

Taken together, the simulation and Device G analyses support the same practical conclusion. Dependence assumptions matter when estimating joint survival, especially under moderate or heavy censoring. The effect is not the same for all dependent models. Copulas provide flexible association between margins [6]; shared frailty captures unobserved measurement-level heterogeneity [8]; and Marshall–Olkin models represent common shocks that can generate simultaneous failures [22,37]. The best model is therefore not simply the most flexible one, but the one whose stochastic mechanism is closest to the failure process being studied. This point is consistent with reliability applications in which censoring and dependence misspecification can materially affect risk assessment [38].

5. Discussion

The simulation study and the Device G application lead to a common message: independence is useful as a reference model, but it should not be treated as a neutral final assumption when the failure process is plausibly dependent. The effect of dependence is not only a matter of parameter estimation. Different dependence mechanisms produce different shapes for the joint survival function

$$S(t_1, t_2) = \Pr\{T^{(1)} > t_1, T^{(2)} > t_2\},$$

and these shapes become more difficult to recover as censoring increases. This is consistent with the competing-risks literature, where the joint distribution of latent failure times is not identified from observed competing-risk data without additional modeling assumptions [3,37]. Recent work on dependent censored competing-risk data reaches a similar conclusion: censoring and dependence must be considered together when estimating reliability or survival quantities [39,40].

The numerical results should therefore be read as evidence about mechanisms, not as a ranking that applies to every reliability problem. In the simulation settings with a common-shock component, the Marshall–Olkin Weibull model performed well because its structure matches the data-generating process. The Marshall–Olkin exponential model was also competitive when the exponential shock assumption was adequate, but it was less flexible when time-varying hazards were present. The independent Weibull model remained a useful benchmark, and in some high-censoring summaries it produced a small aggregate error. This does not imply that independence is preferable under dependence; rather, it shows that heavy censoring can reduce the information needed to distinguish between dependence mechanisms.

The distinction between continuous dependence and common-shock dependence is central. Copula models are useful when the dependence between failure modes is mainly expressed as association between continuous latent times. They preserve the marginal survival models and modify the joint structure through the copula, which makes them attractive in applications where marginal behavior and dependence are best modeled separately [21,41]. The Gumbel and Clayton families used here represent different tail-dependence patterns and provide interpretable alternatives to independence. Related studies on dependent censored and masked competing-risk data also support the use of copulas when association among failure causes is expected but exact simultaneous failures are not the main physical mechanism [39,42].

Marshall–Olkin models have a different interpretation. Their purpose is not only to increase the strength of dependence, but to represent a physical common-shock mechanism. In these models, a shared event can cause both failure modes to occur at the same time, producing a singular component on the diagonal $t_1 = t_2$. This feature cannot be reproduced by an absolutely continuous copula with continuous margins. Thus, MOE and MOW specifications are most appropriate when engineering knowledge, failure records, or inspection data suggest that external shocks, cascading effects, or shared stress events can affect both modes simultaneously [43,44]. In such cases, treating simultaneous failures as ordinary ties may hide a meaningful part of the failure process.

Shared frailty models address another source of dependence: unobserved heterogeneity among measurements. A frailty term is useful when the association between failure modes may arise from differences in manufacturing quality, operating environment, maintenance history, or usage intensity. In that setting, a measurement with a large frailty value is more vulnerable to both modes, whereas a measurement with a small frailty value is less vulnerable to both. This interpretation follows the standard view of frailty as a

latent multiplicative effect on the hazard scale [8,9]. The results also show, however, that frailty should not be used as a generic correction for any form of dependence. If the true mechanism is a common shock, a frailty model may improve over independence but still fail to reproduce the diagonal structure generated by Marshall–Olkin dependence [45].

Censoring has two consequences for model interpretation. First, it reduces the amount of information available for estimating the marginal hazards. Second, it makes the dependence mechanism harder to identify, especially when few failures are observed in one mode or when simultaneous failures are rare. These effects were visible in the simulation results and in the Device G sensitivity analysis. Under moderate and high censoring, the estimated joint survival curves separated more clearly across model classes. This supports the use of dependence models as sensitivity tools: when several plausible mechanisms lead to materially different reliability estimates, model choice should be guided by both statistical diagnostics and knowledge of the failure process.

The likelihood-based estimates must also be interpreted with care. The models considered in this article involve nonlinear likelihoods, constrained parameters, and in the Marshall–Olkin case, singular components. Heavy censoring, boundary estimates, weakly identified dependence parameters, or zero failures in one mode can make the observed information matrix unstable. Computational issues of this type are common in censored competing-risk models and often require numerical likelihood maximization together with simulation checks [46,47]. For this reason, transformed parameters, bounded optimization, multiple starting values, Hessian checks, profile likelihoods, and bootstrap intervals are not merely computational conveniences. They are part of the inferential procedure needed to assess whether the reported estimates are stable and interpretable [19,35].

The marginal model remains equally important. Weibull margins were used because they provide a parsimonious way to represent decreasing, constant, and increasing hazards, which are common in reliability applications [17]. Nevertheless, dependence estimates can be affected by marginal misspecification. For example, if a strongly increasing hazard is forced into an exponential margin, part of the marginal lack of fit may be absorbed by the dependence parameter. The dependence mechanism should therefore be interpreted only after the marginal behavior has been checked. Although this article focuses on exponential and Weibull margins to keep the comparison controlled, finite-support alternatives such as Kies-type distributions and more flexible Weibull extensions may be useful when the physical operating window is bounded or when the marginal hazard shape is more complex [18,48].

The real-data analysis should be viewed in the same spirit. The Device G data do not prove that one dependence model is uniquely correct. Instead, they show that the estimated joint reliability can change when dependence between failure modes is modeled rather than suppressed. This is especially relevant in engineering applications, where the fitted model may influence maintenance planning, warranty decisions, or risk assessment. A model that fits the marginal survival curves well may still give misleading joint reliability estimates if the dependence structure is inconsistent with the underlying failure mechanism.

Several limitations should be acknowledged. The comparison was restricted to two failure modes, parametric margins, selected Archimedean copulas, gamma frailty, and Marshall–Olkin exponential and Weibull specifications. More complex systems may involve more than two modes, covariates, time-dependent stressors, masked causes, or nonparametric marginal components. The simulation grid was designed to compare mechanisms under controlled conditions, not to exhaust all possible reliability settings. These limitations do not weaken the main conclusion; rather, they indicate where the framework can be extended. Future work may incorporate covariates, alternative censoring mechanisms,

Bayesian estimation, finite-support margins, or higher-dimensional Marshall–Olkin and copula structures.

Practical Recommendations by Scenario

The practical workflow should begin with the margins. Before choosing a dependence model, the analyst should fit and diagnose the marginal lifetime models for each failure mode. Residual plots, probability plots, profile likelihoods, and sensitivity to alternative margins are useful at this stage. Only after the marginal behavior is reasonably described should the dependence structure be interpreted.

Independence should then be fitted as a baseline, not as a default conclusion. It provides a transparent reference for likelihood values, joint survival curves, and uncertainty estimates. If the independent model gives results close to the dependent alternatives and there is no engineering evidence of dependence, it may be adequate for routine prediction. If the dependent models produce noticeably different joint survival estimates, independence should be treated as a sensitivity case rather than as the final model.

When failures are not expected to occur exactly at the same time, but the failure times are associated, copulas are a natural first choice. The Gumbel family is useful when upper-tail association is plausible, whereas the Clayton family is useful when lower-tail association is more relevant [32,33]. In this setting, Kendall's τ provides an interpretable scale for comparing dependence strength across copula families.

When the engineering mechanism suggests shared external shocks, cascading events, or simultaneous component failures, Marshall–Olkin models should be considered. The MOE model is appropriate when exponential shock times are reasonable, whereas MOW allows a common Weibull shape and therefore more flexible time-varying hazard behavior. These models are especially relevant when the event vertex $V_j = (1, 1)$ has a direct physical interpretation as a common-shock failure [44,49].

When the main concern is unobserved variability across measurements, shared gamma frailty is more interpretable than a common-shock model. Frailty is appropriate when measurements differ in hidden vulnerability because of manufacturing conditions, environmental exposure, maintenance history, or usage intensity. It is also useful under moderate or high censoring, where unobserved heterogeneity can affect both point estimates and uncertainty quantification [45,50].

Finally, model selection should not be based on a single numerical criterion. This point is particularly relevant for copula-based reliability models, where different validation criteria may lead to different model choices [51]. Likelihood values, IMSE, confidence-band coverage, convergence behavior, boundary estimates, Hessian conditioning, and profile likelihoods should be reviewed together. The preferred model is the one that provides an adequate statistical fit and has a plausible reliability interpretation. This approach links the statistical evidence with the physical failure mechanism and reduces the risk of selecting a model only because it improves an isolated numerical score.

6. Conclusions

This study compared independence, Archimedean copulas, shared gamma frailty, and Marshall–Olkin specifications for estimating the joint survival function in two-mode competing-risks data under censoring. The comparison was carried out under the common observed-data structure defined in Section 2.1, so that differences among models could be interpreted in terms of the assumed dependence mechanism rather than changes in notation, censoring treatment, or estimation target.

The main finding is that the dependence mechanism can materially change the estimated joint survival surface. The independent Weibull model remains useful as a trans-

parent benchmark, but it should not be treated as a neutral final model when the failure process is plausibly dependent. In the simulation study, models whose stochastic mechanism matched the data-generating structure gave more reliable joint survival estimates. In particular, Marshall–Olkin models were effective when common shocks were present because they explicitly include a singular diagonal term for simultaneous failures. Copula models were more appropriate for continuous association between failure times, while shared frailty provided a natural representation of latent measurement-level heterogeneity.

The results also show that censoring affects more than marginal lifetime estimation. As the censoring proportion increases, the available information for distinguishing among dependence mechanisms decreases. This makes model choice more consequential and also more uncertain. For that reason, the reported estimates should be interpreted together with convergence diagnostics, boundary checks, Hessian behavior, profile likelihoods, and bootstrap or profile-based uncertainty intervals when standard asymptotic approximations are questionable.

The Device G analysis illustrates the practical relevance of the framework. Using the same marginal fitting strategy and observed-data structure, different dependence assumptions led to different joint reliability assessments under incomplete follow-up. The application should not be read as proof that one dependence model is universally correct for the device. Rather, it shows how the proposed workflow can be used to examine whether independence, continuous association, latent heterogeneity, or common shocks provide the most plausible description of the observed failure process.

From a reliability perspective, the findings support a sequential modeling strategy. Marginal lifetime models should be diagnosed first. Independence can then be fitted as a baseline. Candidate dependence models should be selected according to the physical failure mechanism: copulas when association is continuous, frailty when unobserved measurement-level variability is plausible, and Marshall–Olkin models when simultaneous failures or common shocks have a meaningful engineering interpretation. The final model should be chosen from both statistical evidence and substantive knowledge of the system, rather than from a single numerical criterion.

Several limitations remain. The study focused on two failure modes, parametric exponential and Weibull margins, selected Archimedean copulas, shared gamma frailty, and Marshall–Olkin exponential and Weibull models. More complex applications may require covariates, time-varying operating conditions, masked causes of failure, semi-parametric margins, bounded-support lifetime distributions, or higher-dimensional dependence structures. Future work should extend the framework in those directions and evaluate it on additional field datasets where the physical source of dependence can be independently assessed.

Overall, the study shows that joint survival estimation under competing risks requires explicit attention to the mechanism generating dependence. Treating dependence as a generic association parameter is often insufficient. Models that reflect the underlying failure process provide more interpretable joint reliability estimates and offer stronger support for maintenance planning, inspection priorities, and risk assessment under censoring.

Author Contributions: Conceptualization, M.C.J.-E., O.E.B.-C. and C.D.C.-Á.; methodology, M.C.J.-E., O.E.B.-C. and C.D.C.-Á.; formal analysis, O.E.B.-C.; writing—original draft preparation, O.E.B.-C. and M.C.J.-E.; writing—review and editing, C.D.C.-Á.; visualization, M.C.J.-E. and C.D.C.-Á.; supervision, O.E.B.-C. and C.D.C.-Á. All authors have read and agreed to the published version of the manuscript.

Funding: This research received no external funding.

Data Availability Statement: The simulation settings and computational workflow used in this study are described in Sections 3 and 4 and Appendix A. The Device G data used for the applied illustration are described in [1]. No new experimental data were generated for this study.

Acknowledgments: The authors acknowledge the Universidad Nacional de Colombia for administrative and technical support. During the preparation of this manuscript, the authors used ChatGPT (version 5.5) for language editing and stylistic refinement. The authors reviewed and edited all outputs and take full responsibility for the content of this publication.

Conflicts of Interest: The authors declare no conflicts of interest. No person or institution other than the authors had any role in the design of the study; in the collection, analysis, or interpretation of the data; in the writing of the manuscript; or in the decision to publish the results.

Appendix A. Simulation Workflow in R

The following R code outlines the simulation workflow used in the Monte Carlo study. The code follows the notation used throughout the article: for each measurement, the latent failure times are $(T_j^{(1)}, T_j^{(2)})$, the censoring time is C_j, the recorded time is

$$Y_j = \min\{T_j^{(1)}, T_j^{(2)}, C_j\},$$

and the event vertex is $V_j \in \mathcal{V}$. The vertex $(1,1)$ is generated only by Marshall–Olkin models, where a common shock can produce exact simultaneous failure. The workflow documents the data-generation and censoring steps used in the simulations; model-specific likelihood maximization follows Algorithm 1. The analyses were implemented in R [36].

Listing A1. R simulation workflow for the dependence models considered in the study.

```
# ------------------------------------------------------------
# Helper functions
# ------------------------------------------------------------

# Weibull rate parameterization:
# S(t) = exp(-lambda * t^beta), so scale = lambda^(-1 / beta)

rweibull_rate <- function(n, beta, lambda) {
stats::rweibull(n, shape = beta, scale = lambda^(-1 / beta))
}

make_observed_data <- function(T1, T2, C) {
Y <- pmin(T1, T2, C)

V1 <- ifelse(
C < T1 & C < T2, 0L,
ifelse(
T1 < T2 & T1 <= C, 1L,
ifelse(
T2 < T1 & T2 <= C, 0L,
ifelse(T1 == T2 & T1 <= C, 1L, NA_integer_)
)
)
)

V2 <- ifelse(
C < T1 & C < T2, 0L,
ifelse(
```

```
T1 < T2 & T1 <= C, 0L,
ifelse(
T2 < T1 & T2 <= C, 1L,
ifelse(T1 == T2 & T1 <= C, 1L, NA_integer_)
)
)
)

data.frame(Y = Y, V1 = V1, V2 = V2)
}

calibrate_censoring_rate <- function(Tmin, target) {
if (target <= 0) return(0)
if (target >= 1) stop("The target censoring proportion must be less than 1.")

objective <- function(rate) {
mean(1 - exp(-rate * Tmin)) - target
}

stats::uniroot(objective, interval = c(1e-8, 1e3))$root
}

apply_random_censoring <- function(T1, T2, target_censoring) {
n <- length(T1)
Tmin <- pmin(T1, T2)

if (target_censoring <= 0) {
C <- rep(Inf, n)
} else {
rate_c <- calibrate_censoring_rate(Tmin, target_censoring)
C <- stats::rexp(n, rate = rate_c)
}

make_observed_data(T1, T2, C)
}

# ------------------------------------------------------------
# Data-generating mechanisms
# ------------------------------------------------------------

# Independent Weibull risks
generate_independent_weibull <- function(n, beta1, lambda1, beta2, lambda2) {
T1 <- rweibull_rate(n, beta = beta1, lambda = lambda1)
T2 <- rweibull_rate(n, beta = beta2, lambda = lambda2)
list(T1 = T1, T2 = T2)
}

# Gumbel or Clayton copula with Weibull margins
generate_copula_weibull <- function(n, family, tau,
beta1, lambda1,
beta2, lambda2) {
if (!requireNamespace("copula", quietly = TRUE)) {
stop("The 'copula' package is required for this generator.")
}

```

```
if (family == "gumbel") {
theta <- 1 / (1 - tau)
cop <- copula::gumbelCopula(param = theta, dim = 2)
} else if (family == "clayton") {
theta <- 2 * tau / (1 - tau)
cop <- copula::claytonCopula(param = theta, dim = 2)
} else {
stop("family must be either 'gumbel' or 'clayton'.")
}

U <- copula::rCopula(n, cop)

T1 <- stats::qweibull(U[, 1],
shape = beta1,
scale = lambda1^(-1 / beta1))
T2 <- stats::qweibull(U[, 2],
shape = beta2,
scale = lambda2^(-1 / beta2))

list(T1 = T1, T2 = T2, theta = theta)
}

# Shared gamma frailty with Weibull margins
generate_gamma_frailty_weibull <- function(n, beta1, lambda1,
beta2, lambda2,
alpha) {
# Shape-rate parameterization: E[Z] = 1, Var[Z] = 1 / alpha
Z <- stats::rgamma(n, shape = alpha, rate = alpha)

T1 <- rweibull_rate(n, beta = beta1, lambda = lambda1 * Z)
T2 <- rweibull_rate(n, beta = beta2, lambda = lambda2 * Z)

list(T1 = T1, T2 = T2, Z = Z)
}

# Marshall-Olkin exponential shocks
generate_moe <- function(n, lambda0, lambda1, lambda2) {
U0 <- stats::rexp(n, rate = lambda0)  # common shock
U1 <- stats::rexp(n, rate = lambda1)  # mode-specific shock 1
U2 <- stats::rexp(n, rate = lambda2)  # mode-specific shock 2

T1 <- pmin(U1, U0)
T2 <- pmin(U2, U0)

list(T1 = T1, T2 = T2, U0 = U0, U1 = U1, U2 = U2)
}

# Marshall-Olkin Weibull shocks with common shape beta
generate_mow <- function(n, beta, lambda0, lambda1, lambda2) {
U0 <- rweibull_rate(n, beta = beta, lambda = lambda0)
U1 <- rweibull_rate(n, beta = beta, lambda = lambda1)
U2 <- rweibull_rate(n, beta = beta, lambda = lambda2)

T1 <- pmin(U1, U0)
T2 <- pmin(U2, U0)
```

```
list(T1 = T1, T2 = T2, U0 = U0, U1 = U1, U2 = U2)
}

# ------------------------------------------------------------
# One simulation scenario
# ------------------------------------------------------------

run_one_replication <- function(n,
generator,
generator_args,
target_censoring) {
latent <- do.call(generator, c(list(n = n), generator_args))

observed <- apply_random_censoring(
T1 = latent$T1,
T2 = latent$T2,
target_censoring = target_censoring
)

observed
}

# Example:
# dat <- run_one_replication(
#   n = 200,
#   generator = generate_mow,
#   generator_args = list(beta = 1.3,
#                         lambda0 = 0.5,
#                         lambda1 = 0.8,
#                         lambda2 = 0.7),
#   target_censoring = 0.30
# )

# ------------------------------------------------------------
# Model fitting and confidence bands
# ------------------------------------------------------------

# The following steps are performed for each fitted model M:
#
# 1. Construct the model-specific likelihood L_M(theta; D_n).
# 2. Maximize the log-likelihood using the multi-start procedure
#    described in Algorithm 1.
# 3. Evaluate S_hat_M(t1, t2) on the grid T.
# 4. Construct Y_e bands by measurement-level bootstrap:
#      a. resample measurements with replacement;
#      b. refit the model in each bootstrap sample;
#      c. compute log{-log S_hat_M(t1, t2)} on the grid;
#      d. obtain simultaneous percentiles over the grid;
#      e. back-transform the bands to the survival scale.
# The functions for likelihood maximization are model-specific and use
# the likelihood terms defined in Section 2 and Algorithm 1.
```

References

1. Meeker, W.Q.; Escobar, L.A.; Pascual F.G. *Statistical Methods for Reliability Data*; John Wiley & Sons: New York, NY, USA, 2021. Available online: https://books.google.com.co/books?id=39ZKEAAAQBAJ (accessed on 20 February 2026).
2. Lawless, J.F. Statistics in reliability. *J. Am. Stat. Assoc.* **2000**, *95*, 989–992. [CrossRef]
3. Pintilie, M. *Competing Risks: A Practical Perspective*; John Wiley & Sons: Chichester, UK, 2006. Available online: https://books.google.com.co/books?id=ZRh2gl-U6isC (accessed on 24 February 2026).
4. Tsiatis, A. A nonidentifiability aspect of the problem of competing risks. *Proc. Natl. Acad. Sci. USA* **1975**, *72*, 20–22. [CrossRef] [PubMed]
5. Yáñez, S.; Brango, H.; Jaramillo, M.C.; Lopera, C.M. Comparación entre riesgos competitivos vía el estimador cópula-gráfico. *Rev. Colomb. Estadística* **2011**, *34*, 231–248.
6. Nelsen, R.B. *An Introduction to Copulas*; Springer: New York, NY, USA, 2006. [CrossRef] [PubMed]
7. Genest, C.; Nešlehová, J.; Quessy, J.-F. Tests of symmetry for bivariate copulas. *Ann. Inst. Stat. Math.* **2012**, *64*, 811–834. [CrossRef]
8. Duchateau, L.; Janssen, P. *The Frailty Model*; Springer: New York, NY, USA, 2008. [CrossRef]
9. Wienke, A. *Frailty Models in Survival Analysis*; Chapman and Hall/CRC Biostatistics Series: Boca Raton, FL, USA, 2010.
10. Marshall, A.W.; Olkin, I. A generalized bivariate exponential distribution. *J. Appl. Probab.* **1967**, *4*, 291–302. [CrossRef]
11. Barnwal, V.; Panwar, M.S. Competing risks analysis for dependent causes using Marshall–Olkin bivariate generalized lifetime family. *Commun. Stat.–Theory Methods* **2022**, *53*, 1212–1240. [CrossRef]
12. Gupta, A.; Ranjan, R.K.; Gupta, A.; Upadhyay, S.K. A Bayes analysis of a dependent competing risk model based on Marshall–Olkin bivariate Weibull distribution. *Int. J. Reliab. Qual. Saf. Eng.* **2023**, *30*, 2250026. [CrossRef]
13. Wang, A.; Chandra, K.; Xu, R.; Sun, J. The identifiability of dependent competing risks models induced by bivariate frailty models. *Scand. J. Stat.* **2015**, *42*, 427–437. [CrossRef]
14. Escobar-Bach, M.; Helali, S. Dependent censoring with simultaneous death times based on the Generalized Marshall–Olkin model. *J. Multivar. Anal.* **2024**, *204*, 105347. [CrossRef]
15. Wang, A.; Guo, Z.; Zhang, Y.; Wu, J. The analysis of semi-competing risks data using Archimedean copula models. *Stat. Neerl.* **2024**, *78*, 191–207. [CrossRef]
16. Marshall, A.W.; Olkin, I. *Life Distributions*; Springer: New York, NY, USA, 2007. Available online: https://link.springer.com/book/10.1007/978-0-387-68477-2 (accessed on 28 February 2026).
17. Johnson, N.L.; Kotz, S.; Balakrishnan, N. *Continuous Univariate Distributions, Volume 1*, 2nd ed.; John Wiley & Sons: New York, NY, USA, 1994. Available online: https://books.google.com/books?id=pp3BEQAAQBAJ (accessed on 20 February 2026).
18. Zaevski, T.; Kyurkchiev, N. On some mixtures of the Kies distribution. *Hacet. J. Math. Stat.* **2024**, *53*, 1453–1483. [CrossRef]
19. van der Vaart, A.W. *Asymptotic Statistics*; Cambridge University Press: Cambridge, UK, 1998. Available online: https://books.google.com.co/books?id=Ocg2AAAAQBAJ (accessed on 24 February 2026).
20. Yáñez, S.; Escobar, L. A.; González, N. Characteristics of two competing risks models with Weibull distributed risks. *Rev. Acad. Colomb. Cienc. Exactas Físicas Nat.* **2014**, *38*, 298–311. [CrossRef]
21. Joe, H. *Dependence Modeling with Copulas*; Chapman and Hall/CRC: Boca Raton, FL, USA, 2014. Available online: https://books.google.com.co/books?id=09ThAwAAQBAJ (accessed on 24 February 2026).
22. Hougaard, P. *Analysis of Multivariate Survival Data*; Springer: New York, NY, USA, 2012. Available online: https://books.google.com.co/books?id=VJfzBwAAQBAJ (accessed on 28 February 2026).
23. Marshall, A.W.; Olkin, I. A multivariate exponential distribution. *J. Am. Stat. Assoc.* **1967**, *62*, 30–44. [CrossRef]
24. Genest, C.; Rivest, L.P. Statistical inference procedures for bivariate Archimedean copulas. *J. Am. Stat. Assoc.* **1993**, *88*, 1034–1043. [CrossRef]
25. Kundu, D.; Basu, S. Analysis of incomplete data in presence of competing risks. *J. Stat. Plan. Inference* **2000**, *87*, 221–239. [CrossRef]
26. Kundu, D.; Dey, A.K. Estimating the parameters of the Marshall–Olkin bivariate Weibull distribution by EM algorithm. *Comput. Stat. Data Anal.* **2009**, *53*, 956–965. [CrossRef]
27. Bemis, B.M.; Bain, L.J.; Higgins, J.J. Estimation and hypothesis testing for the parameters of a bivariate exponential distribution. *J. Am. Stat. Assoc.* **1972**, *67*, 927–929. [CrossRef]
28. Kundu, D. On hybrid censored Weibull distribution. *J. Stat. Plan. Inference* **2007**, *137*, 2127–2142. [CrossRef]
29. Pareek, B.; Kundu, D.; Kumar, S. On progressively censored competing risks data for Weibull distributions. *Comput. Stat. Data Anal.* **2009**, *53*, 4083–4094. [CrossRef]
30. Mokhtari, E.B.; Rad, A.H.; Yousefzadeh, F. Inference for Weibull distribution based on progressively type-II hybrid censored data. *J. Stat. Plan. Inference* **2011**, *141*, 2824–2838. [CrossRef]
31. Kendall, M.G. A new measure of rank correlation. *Biometrika* **1938**, *30*, 81–93. [CrossRef]
32. Gumbel, E.J. Bivariate exponential distributions. *J. Am. Stat. Assoc.* **1960**, *55*, 698–707. [CrossRef]
33. Clayton, D.G. A model for association in bivariate life tables and its application in epidemiological studies of familial tendency in chronic disease incidence. *Biometrika* **1978**, *65*, 141–151. [CrossRef]

34. Vaupel, J.W.; Manton, K.G.; Stallard, E. The impact of heterogeneity in individual frailty on the dynamics of mortality. *Demography* **1979**, *16*, 439–454. [CrossRef]
35. Nocedal, J.; Wright, S.J. *Numerical Optimization*; Springer Series in Operations Research and Financial Engineering; Springer: New York, NY, USA, 2006. [CrossRef]
36. R Core Team. *R: A Language and Environment for Statistical Computing*; R Foundation for Statistical Computing: Vienna, Austria, 2025. Available online: https://www.R-project.org/ (accessed on 29 June 2026).
37. Kalbfleisch, J.D.; Prentice, R.L. *The Statistical Analysis of Failure Time Data*; John Wiley & Sons: Hoboken, NJ, USA, 2002. Available online: https://books.google.com.co/books?id=38C_DwAAQBAJ (accessed on 3 March 2026).
38. Hong, Y.; Meeker, W.Q. Confidence interval procedures for system reliability and applications to competing risks models. *Lifetime Data Anal.* **2014**, *20*, 161–184. [CrossRef] [PubMed]
39. Salem, M.M. Bayesian analysis for dependent progressively censored Weibull competing risks using copulas. *Int. J. Reliab. Qual. Saf. Eng.* **2023**, *30*, 2350020. [CrossRef]
40. Zhou, X.-D.; Wang, Y.-J.; Wu, L.; Yue, R.-X. Data analysis for accelerated life tests via Weibull-gamma frailty regression models. *Appl. Stoch. Model. Bus. Ind.* **2023**, *39*, 567–583. [CrossRef]
41. Guloksuz, C.T. A study on modelling of bivariate competing risks with Archimedean copulas. *Arch. Curr. Res. Int.* **2021**, *21*, 14–21. [CrossRef]
42. Li, Y.; Ye, J. Analysis for partially accelerated dependent competing risks model with masked data based on copula function. *Commun. Stat.-Simul. Comput.* **2024**, *53*, 1020–1036. [CrossRef]
43. Zuo, Z.; Wang, L.; Lio, Y. Reliability estimation for dependent left-truncated and right-censored competing risks data with illustrations. *Energies* **2023**, *16*, 62. [CrossRef]
44. Brango, H.; Guerrero, A.; Llinás, H. Marshall–Olkin bivariate Weibull model with modified singularity (MOBW$-\mu$): A study of its properties and correlation structure. *Mathematics* **2024**, *12*, 2183. [CrossRef]
45. Gorfine, M.; Zucker, D.M. Shared frailty methods for complex survival data: A review of recent advances. *Annu. Rev. Stat. Its Appl.* **2023**, *10*, 51–73. [CrossRef]
46. Czado, C.; Van Keilegom, I. Dependent censoring based on parametric copulas. *Biometrika* **2023**, *110*, 721–738. [CrossRef]
47. Alotaibi, R.; Nassar, M.; Elshahhat, A. Statistical Computation of Hjorth Competing Risks Using Binomial Removals in Adaptive Progressive Type II Censoring. *Mathematics* **2025**, *13*, 2010. [CrossRef]
48. Xu, M.; Mao, H. q-Weibull distributions: Perspectives and applications in reliability engineering. *IEEE Trans. Reliab.* **2025**, *74*, 3112–3125. [CrossRef]
49. Prajapati, D.; Ling, M.H.; Shing Chan, P.; Kundu, D. Misspecification of copula for one-shot devices under constant stress accelerated life-tests. *Proc. Inst. Mech. Eng. Part O J. Risk Reliab.* **2023**, *237*, 725–740. [CrossRef]
50. Zhang, L.; Yan, R. Copula-based reliability estimation of parallel-series system in the multicomponent stress–strength dependent model. *Probab. Eng. Informational Sci.* **2025**, *39*, 309–325. [CrossRef]
51. Bru, O.E.; Martínez, M.A.; Correa-Alvarez, C.D. Selección de cópulas mediante validación cruzada: Un estudio de simulación. *Cienc. Desarro.* **2025**, *16*, 94–106. [CrossRef]

Disclaimer/Publisher's Note: The statements, opinions and data contained in all publications are solely those of the individual author(s) and contributor(s) and not of MDPI and/or the editor(s). MDPI and/or the editor(s) disclaim responsibility for any injury to people or property resulting from any ideas, methods, instructions or products referred to in the content.